arXiv:1512.04451v1 [astro-ph.SR] 14 Dec 2015

# Spectropolarimetry of Atomic and Molecular Lines near 4135nm

M Penn, H Uitenbroek, TA Clark, R Coulter, PR Goode, W Cao
National Solar Observatory
950 N Cherry Av, Tucson AZ 85726
email: mpenn@nso.edu
http://www.noao.edu/noao/staff/mpenn/

12 Oct 2015

**Abstract**

New spatially scanned spectropolarimetry sunspot observations are made of photospheric atomic and molecular absorption lines near 4135nm. The relative splittings among several atomic lines are measured and shown to agree with values calculated with configuration interaction and intermediate coupling. Large splitting is seen in a line identified with Fe I at 4137nm, showing multiple Stokes V components and an unusual linear polarization. This line will be a sensitive probe of quiet Sun magnetic fields, with a magnetic sensitivity of 2.5 times larger than that of the well-known 1565nm Fe I line.

# 1 Introduction

Measurements of solar magnetic fields are essential to modern research efforts, and newly built telescopes and their instruments (i.e. NST and CYRA, Cao *et al.* (2010)) and telescopes and instruments currently under construction (i.e. DKIST and Cryo-NIRSP, Lin (2003)) have new infrared magnetic observations in their core science programs. Historically measurements of magnetic fields at infrared wavelengths have enabled new scientific advances in solar physics, and these instruments intend to capitalize on such observations and seek new infrared tools as well. It is well-known that for solar spectral lines with identical magnetic splitting, the relative sensitivity of lines to solar magnetic fields increases with increasing wavelength. As a method to determine which spectral lines to target for increased accuracy in measuring the solar magnetic field, the concept of the magnetic resolution of a spectral line can be used. The magnetic sensitivity is determined by the ratio of the magnetic Zeeman splitting $\lambda^2 g_{eff}$ and the Doppler line broadening $\lambda$ and thus varies as $\lambda g_{eff}$. Currently the most sensitive probes of the solar magnetic field include the Fe I 1564.8nm spectral line ($\lambda g_{eff} = 4695$) for photospheric fields, the Ti I 2233nm line ($\lambda g_{eff} = 5778$) for fields in cold sunspot umbrae, and the Mg I 12381nm line ($\lambda g_{eff} = 12318$) for penumbral and plage magnetic fields. Reports of other very sensitive spectral lines near 4135nm have been made but no measurements have been published.

Identification of infrared lines is still a challenging task, and several lines remain unidentified even today (Geller, 1995). From laboratory work, lines from high-energy transitions in Fe I, in particular from the $3d^6 4s6s$ to $3d^6 4s6p$ configurations have "...fragmented analysis with only a few lines known." (Johansson and Cowley, 1988) For lines in the 4135nm region, only one identification is given by Nave *et al.* (1994) for the 4136.4908 nm line. The energy levels for the transition correspond to 56541.592 $cm^{-1}$ and 54124.740 $cm^{-1}$ for the upper and lower levels, respectively, producing a transition at 2416.86 $cm^{-1}$ or 4136.48579nm. The electronic configurations and terms listed by Nave *et al.* (1994) are $3d^6 4s(^6D)6p(^7P^0)$ and $3d^6 4s(^6D)6s(g^7D)$ for the upper and lower levels. Using L-S coupling (e.g. Beckers (1969)) to determine the magnetic sensitivity of this transition gives $g_{eff} = 1.70$.

Using theoretical models and fitting to laboratory spectra, Kurucz (2011) has published a set of infrared line identifications with electron configurations and terms for the upper and lower levels for these lines, as well as the Lande-g values for the levels for the lines from Fe I (Kurucz, 2011). These calculations differ from previous work in that the energy levels are not specifically assigned to an individual electronic configuration and term, but rather to a superposition of overlapping configurations. These configuration interactions are solved to produce an eigenvector of electronic states with a set of contribution coefficients for each state. The energy level is then composed of the sum of these individual levels. With a mixture of electronic configurations for the upper and lower states of the 4136.5nm transition, LS coupling is applied to each possible combination of upper and lower states weighted with the proper coefficients to produce a value for the magnetic sensitivity of the spectral line; this calculation is called intermediate coupling. For the Fe I 4136.5nm line the computed value for intermediate coupling is $g_{eff} = 1.62$. While intermediate coupling gives a similar value to LS coupling in this example, this is not always the case.

To determine the relative importance of mixed terms for the energy levels which produce a particular spectral line, the Zeeman splittings of spectral lines measured in the laboratory can be compared against the predictions from both L-S and intermediate coupling (Curtis, 2003). The observations presented in this work provide the first such experimental data from the Sun which can be used to address such questions about several spectral lines near 4135nm. Furthermore, the polarized spectral line profiles observed in sunspots and presented in this paper will provide an experimental constraint on the intermediate coupling theory used to compute the Lande-g values. While the values of $g_{eff}$ have been computed for intermediate coupling, the polarized spectral line profiles themselves have not been computed. These profiles are critical for using these spectral lines

to infer the magnetic fields on the Sun. They can be computed by first computing the expected LS coupling Zeeman patterns among all the configuration interaction levels, and then weighting those patterns with the proper coefficients.

In section 2 we review the atomic levels the relevant atomic and molecular lines near 4135nm, in section 3 we discuss new solar observations of this part of the spectrum, and then in section 4 we present the wavelengths and magnetic splittings measured for these lines.

## 2 Lines near 4135nm

Observations of the quiet Sun photospheric spectrum near 4135nm were made from space during the ATMOS experiment (Farmer and Norton, 1989) and from the ground at the National Solar Observatory's McMath/Pierce Solar Facility (McM/P) (Wallace and Livingston, 2003). Observations of the sunspot umbral spectrum near 4135nm were also made at the McM/P ( Wallace *et al.* (2002) and Wallace and Livingston (1992)). Line identifications are given in the McM/P spectra, and have been made for the ATMOS spectra too (Geller, 1992).

Table 1 lists the observed atomic spectral lines in this part of the solar spectrum as seen in the quiet Sun photosphere. Here the first wavelength values (with the K subscript) are taken from Kurucz (2011), as are the values for $log(gf)$. The second wavelength values and the line depth values (with the G subscript) are taken from Geller (1992), and here the line depths have been converted to continuum percentages. Finally, the last two columns (with the NAC subscript) represent recent observations taken from the McM/P and will be described in more detail in the following section.

Table 1: Atomic Spectral lines

| Species | $\lambda_K$ [nm] | log(gf) | $\lambda_G$ [nm] | $\text{Depth}_G$ | $\lambda_{NAC}$ [nm] | $\text{Depth}_{NAC}$ |
|---|---|---|---|---|---|---|
| Si I | 4122.8421 | -2.190 | 4122.79 | 3.2 | 4122.90 | 0.6 |
| Si I | 4132.7169 | 0.250 | 4132.72 | 16.0 | 4132.75 | 5.2 |
| Fe I | 4136.4857 | 0.512 | 4136.47 | 7.9 | 4136.50 | 2.7 |
| Fe I | 4137.0095 | -1.630 | 4136.97 | 3.1 | 4136.99 | 0.8 |
| Fe I | 4139.2294 | 0.448 | 4139.18 | 6.8 | 4139.19 | 2.6 |
| Si I | 4142.5516 | 0.580 | 4142.47 | 9.6 | 4142.48 | 5.2 |

The infrared solar spectrum has few atomic lines, and the lines that are present are often weak. In order to produce lines at these wavelengths, the energy difference between the upper and lower levels must be small. The energy difference between levels near the ground state of most atoms is larger, resulting in lines in the UV or visible. Only as one moves to higher excited states does one find upper and lower levels with relatively close spacing in energy which are able to produce spectral features in the infrared. For both Fe I and Si I, the upper and lower energy levels for these lines are rather close to the ionization energies, which are about 63737 $cm^{-1}$ for Fe I (Sugar and Corliss, 1985) and 65748 $cm^{-1}$ for Si I (Martin and Zalubas, 1983). As the temperature of the solar plasma drops from the value in the quiet Sun to lower values in sunspots, the electron populations in these energy levels are much smaller. For this reason the strength of these absorption lines is greatly reduced in sunspots, and these spectral lines are not useful tools for examining the physical conditions in sunspot umbrae. In the penumbrae of sunspots, it is expected that the lines are probing the physical conditions in the hotter plasma, or brighter penumbral structures. It is expected that these spectral lines will prove most useful as diagnostics for the quiet Sun plasma.

Table 2 lists the energy levels involved with each of these lines, and the primary level configurations for each level (although it is important to remember that other configurations are important under the condition of configuration interaction). The identifications are taken from Geller (1992) and Wallace and Livingston (2003), with the exception of the 4137nm line, which is here associated with an Fe I transition listed by Kurucz (2011). Electron configuration and terms for Si I were taken from Martin and Zalubas (1983) and they report mixing percentages for configuration interactions in the energy levels at 54871, 56690, and 58893 $cm^{-1}$. For Fe I the configurations and terms were taken from Nave *et al.* (1994). For these primary configurations, the values for the L,S and J quantum numbers are listed, along with the Lande g value (from Kurucz (2011)) for the energy levels.

Table 2: Line Identifications

| Species | $\lambda_K$ [nm] | Level Energy [$cm^{-1}$] | Level Configuration (primary) | Level $g_K$ |
|---|---|---|---|---|
| Si I | 4122.8421 | 54871.031 | $3s^2 3p5s\ ^1P^0$ | |
| | | 57295.881 | $3s^2 3p5p\ ^3P$ | |
| Si I | 4132.7169 | 56690.903 | $3s^2 3p4d\ ^3P^0$ | |
| | | 59109.959 | $3s^2 3p(^2P^0_{3/2})4f\ ^2[5/2]$ | |
| Fe I | 4136.4857 | 54124.740 | $3d^6 4s(^6D)6s\ g^7D$ | 1.650 |
| | | 56541.592 | $3d^6 4s(^6D)6p\ ^7P^0$ | 1.587 |
| Fe I | 4137.0095 | 54747.594 | $3d^6 4s(^6D)6s\ g^7D$ | 2.999 |
| | | 57164.140 | $3d^6 4s(^6D)6p\ ^7D^0$ | 2.642 |
| Fe I | 4139.2294 | 54611.706 | $3d^6 4s(^6D)6s\ g^7D$ | 1.997 |
| | | 57026.956 | $3d^6 4s(^6D)6p\ ^7F^0$ | 1.659 |
| Si I | 4142.516 | 58893.400 | $3s^2 3p4d\ ^1F^0$ | |
| | | 61306.713 | $3s^2 3p(^2P^0_{1/2})5f\ ^2[7/2]$ | |

For the case of LS coupling, the Landé g value for the energy level can be given with the well-known expression (e.g. Beckers (1969) equation 1) and then the value for $g_{eff}$ for the spectral line can be computed from the values for the upper and lower levels as: (Beckers (1969) equation 6): $g_{eff} = \frac{1}{8}(J_u - J_l)(J_u + J_l + 1.0)(g_u^2 - g_l^2)$.

The molecular lines in this region of the spectrum are dominated by OH and SiO lines. Geller (1992) lists several OH lines in this part of the spectrum as observed from the ATMOS data at wavelengths of 4133.26, 4135.10, 4136.79 and 4142.69nm. In this spectral region, Wallace *et al.* (2002) identify about 30 lines from SiO, and three lines from CO. They also identify 7 OH lines, including all of the OH lines from Geller (1992) plus new identifications at roughly 4136.5 , 4137.9 and 4139.2nm.

# 3 Observations and Data Analysis

Two sets of observations have been used to investigate these spectral lines, both taken at the 1.6m diameter McM/P main telescope and main spectrograph (Pierce, 1964), but using two different

instruments. The first measurements were taken with the NIM instrument (Rabin *et al.*, 1992) and measured the intensity profiles across several sunspots in the late 1990's. The more recent measurements were taken using the the NSO Array Camera (NAC) with a 1024 x 1024 InSb Alladin 3 array as the detector. While the NIM observations include several additional lines of interest, including lines at 4056 and 4122.8nm, and while the NIM observations were the inspiration for the recent NAC observations, here only the NAC observations will be discussed, and in future work more details of the NIM observations will be presented.

In the NAC observations, the wavelength selection in the dewar was done using a 1-inch round cold filter (at roughly 60K) with a 18 nm bandpass centered at 4137 nm with a peak transmission of 75 %. Since the main spectrograph is warm, the observations contain a large background level. Exposure times were 25 microseconds per frame. The McMath-Pierce optics are expected to produce a very small instrumental polarization at this wavelength, and the polarization crosstalk cannot be measured with this data.

The polarization analysis for the NAC observations was done using optics positioned at the spectrograph exit port. A reimaging bench using two CaF2 lenses collimated the spectrograph exit and reimaged it onto the NAC detector. A rotating waveplate was positioned at the spectrograph exit focal plane, and then a linear polarizer was used in the collimated beam. Since the rotating waveplate is positioned near an image plane, deflection of the beam is not an issue, but dust and other transmission features on the waveplate are challenging to remove during calibration. A slow-chopping method was used by rotating the waveplate between exposures. For sunspot scans, a scanning mirror stepped the solar image perpendicular to the spectrograph slit at the end of a sequence of polarization exposures. Background and flat field corrections were made for each exposure at the waveplate positions. The waveplate rotations positions were calibrated using a second linear polarizer in the beam.

Table 3 lists details of both the NIM and the NAC observations.

Table 3: McM/P Observations

| Number | Date | Time [UT] | Wavelength [nm] | Sunspot | Stokes type |
|---|---|---|---|---|---|
| 1 | 2013/05/02 | 21:08 | 4120-4145 | NOAO 11777 | I |
| 2 | 2013/09/05 | 21:10 | 4136-4139 | NOAO 11836 | I,V |
| 3 | | 21:22 | 4132-4136 | NOAO 11837 | I,V |
| 4 | | 21:29 | 4136-4139 | NOAO 11838 | I,V |
| 5 | 2013/09/12 | 17:07 | 4136-4139 | NOAO 11841 | I,Q,U,V |
| 6 | 2013/09/25 | 18:31 | 4136-4139 | NOAO 11846 | I,Q,U,V |

Because the McM/P adaptive optics system was not used for these observations, the solar pointing of different waveplate sequences is not stable. Only exposures where two or more spectral lines are simultaneously measured are used to compute the relative splitting ratios between lines, in this way the magnetic fields sampled by the different lines is identical and the different splitting represent the inherently different responses from the spectral lines. The NAC exposure times and the waveplate rotation were run in open-loop mode, resulting in some overhead time where photons were not collected.

# 4 The Intensity and Polarization Spectra

## 4.1 Intensity Spectra 4120-4145nm

The four strongest lines in this spectral region are two each from Fe I and Si I. There are also two weaker lines, one each from Fe I and Si I. There are also several telluric absorption lines. The spectra are shown in Figure 1. The averaged NAC spectrum has about 10 times better signal to noise than in the spectrum from Wallace and Livingston (2003) but the lines appear weaker in the NAC spectrum due to the reduced spectral rsolution compared to Wallace and Livingston (2003). Many frames were stitched together to produce this spectrum, where each single NAC image covers about 4nm of the solar spectrum.

The wavelength calibration of this data was done using a set of six telluric absorption lines located at 4131.79, 4133.15, 4134.69, 4137.94, 4141.03, and 4144.12nm as measured in the Wallace and Livingston (2003) No corrections were made for the Doppler shift caused by the relative motion of the Sun and the telescope, nor for the gravitational redshift of the Sun. As shown in Table 1, the three Si I line centers were measured at positions of 4122.90, 4132.75 and 4142.48nm and the three Fe I line centers were measured to be at 4136.50, 4136.99 and 4139.19nm. The uncertainty in these observed wavelengths is about ±0.005nm.

The observed line depths from the NAC observations correlates well with the line depths from ATMOS (Geller, 1992) with the exception of the 4142nm Si I line. The NAC line depths are roughly one-third of the ATMOS line depths, except that in the NAC observations the 4142nm line is about twice as deep as this relationship would suggest.

Figure 2 shows a spectral frame from the 25 Sep 2013 observations; in this frame, the upper and lower sections of the slit show the quiet Sun spectrum, the middle of the slit crosses a sunspot umbra and the other parts of the slit show signal from the penumbral regions. The spectral range covers from about 4136 to 4141nm. This frame was produced by averaging the spectrum from 240 individual exposures, after each was shifted to align the sunspot position along the slit. Residual seeing motions perpendicular to the slit were not corrected, and so some spatial smearing is introduced. The umbral regions of this sunspot show a continuum brightness of about 0.72 times the quiet Sun brightness. As shown in Figure 2, there are several spectral lines which are not present in the quiet Sun regions, but appear in the sunspot umbral regions. They are identified using Wallace *et al.* (2002). The strongest molecular lines seen in the intensity spectrum are at the following measured wavelengths: 4136.48 (OH or SiO), 4136.85 (SiO), 4137.48 (SiO or CO), 4137.98 (OH), 4138.54 (SiO), 4139.40 (OH), 4139.63 (SiO), and 4140.75 (SiO). In all cases the error in the line center wavelengths is estimated to be about ±0.02nm. The only ATMOS molecular identifications in this range listed in Geller (1992) are from OH at 4136.79 and 4139.26nm and these lines are not seen in the sunspot spectra of Wallace *et al.* (2002), nor in these NAC sunspot spectra.

## 4.2 The Polarization Spectrum 4135-4139nm

The Stokes spectra of these lines show a wealth of detail. In Figure 3, a Stokes V spectral frame is shown; this corresponds to the same position as the Stokes I frame shown in Figure 2. This and subsequent Stokes Q and Stokes U frames are made by analyzing 30 waveplate rotations, each of which was sampled with 8 exposures. As in the Stokes I spectral frame, motion of the sunspot along the slit was corrected, but motion perpendicular to the slit will add spatial smearing, and possibly spectral broadening as slightly different magnetic fields are sampled in each exposure. It is important to note that all three spectral lines are impacted in identical ways, since they all appear on the same spectral frame. This frame prominently shows the circular polarization signature from the three Fe I spectral lines, as well as the spectra from four molecular lines confined to the sunspot umbra.

The averaged spectral frame shown in Figure 3 reveals that the McM/P observations from the NAC currently lack the signal to noise needed to measure the magnetic fields in the quiet Sun outside of the penumbra. The spectral lines sample the penumbral fields well, but when the field strength increases some of the Zeeman components from 4136 and 4137 blend. The lines are very weak in the sunspot umbra, and do not seem useful for measuring the magnetic fields there.

In order to examine the relative magnetic splittings, the NAC Stokes V profiles were examined using a number of techniques. The analysis was restricted to only spectral frames showing two or more lines; in this way the spectral lines are identically affected by seeing conditions, and the spectral lines sample the identical solar magnetic fields. The splitting was examined by eye using spectral profiles, and then the Stokes signals in several frames were examined by hand. Another more detailed analysis involved finding the wavelength positions of the Stokes V $\sigma$ spectral components at several slit positions, and fitting a polynomial function to these splittings to derive the splittings along the whole slit. In most cases both $\sigma$ components were used for these measurements, however when the components were blended or outside of the spectral frame, one component was measured relative to the line center position.

The measured splittings for all the lines were then compared to the splitting of the Fe I 4139nm splitting. The results are presented in Table 4. The sources of error to consider in these measurements are the uncertainty in the wavelength position of the $\sigma$ component (small) the spatial scatter in the ratio of the splitting in well-measured penumbral regions (reported in Table 4), and the uncertainty in the line center position in cases where only one $\sigma$ component is measureable (difficult to quantify, but estimated to be small).

From Stenflo (1994) the Zeeman splitting of a line $\Delta\lambda = 4.6710^{-13} g_{eff} \lambda^2 B$, where $B$ is the solar magnetic field causing the splitting. Here we ignore the 0.2% changes due to the different wavelengths of the lines and set $\lambda$ for each line equal. As long as the magnetic field being measured is identical (a condition which is satisfied if the lines are in the same spectral image) then we can compute the ratio of the $g_{eff}$ values for each line as the ratio of the observed splittings $\frac{g_{4136}}{g_{4139}} = \frac{\Delta\lambda_{4136}}{\Delta\lambda_{4139}}$.

The splitting for the Fe I 4137nm line is a special case, since as revealed by Figure 3, the line seems to display multiple $\sigma$ components in the Stokes V spectrum. The individual components are split by factors of 1.44 $\pm$ 0.05 and 2.55 $\pm$ 0.23 respectively. The amplitude ratio of the two components is difficult to measure, but is estimated at 1.75 $\pm$ 0.25, with the component with the larger shift having the weaker Stokes V amplitude. Using the averaging technique described by Beckers (1969) the Lande factor for this line is then determined to be $g_{eff}$= 1.84$\pm$0.21.

Table 4: Zeeman Line Splittings Relative to Fe I 4139nm

| Atom | Wavelength [nm] | Kurucz Ratio (vs 4139nm) | Measured Ratio (vs 4139nm) |
|---|---|---|---|
| Si I | 4132.7 | | 1.00$\pm$0.12(3) |
| Fe I | 4136.5 | 1.23 | 1.12$\pm$0.67 (2) |
| | | | 1.28$\pm$0.14 (4) |
| | | | 1.39$\pm$0.07 (5) |
| | | | 1.32$\pm$0.03 (6) |
| Fe I | 4137.0 | 2.13 | 1.84$\pm$0.21 (6) |

Four of the molecular lines seen in the sunspot from 20130925 show strong Stokes V profiles. These are the lines at: 4136.48 (OH or SiO) 4136.85 (SiO) 4137.98 (OH) and 4139.40nm (OH). The lines at 4136.48 and 4137.98nm show a Stokes V profiles which has the opposite sense of the atomic and the other molecular lines: these transitions have a negative $g_{eff}$.

None of the molecular lines show completely resolved splitting profiles in the sunspot umbra,

rather they resemble the types of unresolved Stokes V profiles seen in weak magnetic fields. Using the weak field approximation, we can compare the relative $g_{eff}$ of the lines by examining the amplitudes of the Stokes I derivatives and Stokes V profiles of the lines. From Stenflo (1994) when the Zeeman splitting of a line is weaker than the Doppler broadening, the Stokes V signal can be approximated by $V(\lambda) \approx B g_{eff} \frac{\partial I}{\partial \lambda}$ where $B$ is the solar magnetic field causing the splitting. Again, as long as the magnetic field being measured is identical (a condition which is satisfied if the lines are in the same spectral image) then we can compute the ratio of the $g_{eff}$ values for line 1 compared to line 2 as the ratio of: $\frac{g_1}{g_2} = \frac{V_1}{V_2} \frac{\partial I_2/\partial \lambda}{\partial I_1/\partial \lambda}$. In Table 5 we list the ratios of the Stokes I derivatives and V amplitudes of the lines, normalizing all of the lines by the ratio of the OH line at 4139.63nm. While the Stokes I derivatives for these lines are within a few percent of each other, there are larger differences in the Stokes V amplitudes. The measurement errors in these relative values are small, but the systematic errors caused by an uncertain background subtraction are estimated at the level of 10%. In the two cases where the molecules show an inverted Stokes V profile, the ratio is listed as negative. From the values in the Table it is clear that the SiO line at 4136.85nm has the largest value for $g_{eff}$ of all four of these lines.

Table 5: Stokes V Amplitudes Relative to OH 4139.63nm

| Molecule | Wavelength [nm] | $\partial I/\partial \lambda$ (vs 4139.63nm) | Stokes V (vs 4139.63nm) | $g_{eff}$ ratio (vs 4139.63nm) |
|---|---|---|---|---|
| OH (or SiO) | 4136.48 | 1.04 | -0.8 | -0.77 |
| SiO | 4136.85 | 0.98 | 1.25 | 1.28 |
| OH | 4137.98 | 1.05 | -0.8 | -0.77 |

The Stokes Q and U polarization profiles are very strange for the Fe I 4137nm spectral line. Both the 4136nm and 4139nm Fe I lines show typical linear polarization profiles with central $\pi$ components and magnetically shifted $\sigma$ components. For both lines the $\sigma$ components have the same polarity at a given spatial location in the penumbra. However, the 4137nm line is different. First, there is no unshifted central $\pi$ component in the Stokes Q or Stokes U profile. Secondly, the magnetically split $\sigma$ components are visible, but they have the opposite polarity as the $\sigma$ components for the 4136 and 4139nm lines. This is unexpected, especially since the Stokes V profiles for all three Fe I lines show the same polarity for the magnetically shifted $\sigma$ components. The molecular absorption lines in the sunspot umbra seem to show no signals in the linear polarization Stokes Q and Stokes U data.

# 5 Conclusions

The identifications of these infrared solar spectral lines with particular transitions in Fe I and Si I is difficult, but the latest observations from the NSO McM/P using the NAC confirms several identifications made by Kurucz. Relative to the Fe I line at 4139nm, the Zeeman splitting of the 4136nm line is $1.28 \pm 0.17$, consistent with the prediction from the intermediate coupling model. The Zeeman splitting of the Fe I line at 4137nm shows two components, with an intensity averaged splitting about 2 times the 4139nm line splitting; this is roughly consistent with the value predicted from the intermediate coupling. The magnetic sensitivity of this line is therefore very high, with a $\lambda g_{eff} = 11600$. While these lines may be useful for sunspot penumbra observations, their main advantage will be realized with future observations with lower backgrounds where they will be a critically useful diagnostic of quiet Sun magnetic fields.

## 6 Acknowledgements

Thanks to Robert Kurucz for clarifying discussions.

# References


Beckers, J. M., 1969, *A table of Zeeman Multiplets*, Sacramento Peak Observatory Contribution no.141 - Physical Science Research Papers no. 371, Sacramento Peak Observatory and Air Force Cambridge Research Laboratories, Sacramento. [ADS]

Cao, W., Gorceix, N., Coulter, R., Ahn, K., Rimmele, T. R. and Goode, P. R., 2010, "Scientific instrumentation for the 1.6 m New Solar Telescope in Big Bear", *Astronomische Nachrichten*, **331**, 636. [DOI], [ADS]

Curtis, L.J., 2003, *Atomic Structure and Lifetimes: A Conceptual Approach*

Farmer, C. B. and Norton, R. H., 1989, *A high-resolution atlas of the infrared spectrum of the sun and the earth atmosphere from space. A compilation of ATMOS spectra of the region from 650 to 4800 $cm^{-1}$ (2.3 to 16 $\mu m$). Vol. I. The sun.*. [ADS]

Geller, M., 1992, *A High-Resolution Atlas of the Infrared Spectrum of the Sun and the Earth Atmosphere from Space Volume III. Key to Identification of Solar Features*

Geller, M., 1995, "Line Identification in ATMOS Solar Spectra", in *Laboratory and Astronomical High Resolution Spectra*, (Eds.) Sauval, A. J., Blomme, R., Grevesse, N., Astronomical Society of the Pacific Conference Series, 81, [ADS]

Johansson, S. and Cowley, C. R., 1988, "Complex atoms in astrophysical spectra", *Journal of the Optical Society of America B Optical Physics*, **5**, 2264–2279. [DOI], [ADS]

Kurucz, R. L., 2011, "Including all the lines", *Canadian Journal of Physics*, **89**, 417–428. [DOI], [ADS]

Lin, H., 2003, "ATST near-IR spectropolarimeter", in *Innovative Telescopes and Instrumentation for Solar Astrophysics*, (Eds.) Keil, S. L., Avakyan, S. V., Society of Photo-Optical Instrumentation Engineers (SPIE) Conference Series, 4853, [ADS]

Martin, WC and Zalubas, R., 1983, "Energy Levels of Silicon, Si I through Si XIV", *Journal of Physical and Chemical Reference Data*, **12**, 323–380

Nave, G., Johansson, S., Learner, R. C. M., Thorne, A. P. and Brault, J. W., 1994, "A new multiplet table for Fe I", *Astrophysical Journal Supplement*, **94**, 221–459. [DOI], [ADS]

Pierce, A. K., 1964, "The McMath solar telescope of Kitt Peak National Observatory", *Applied Optics*, **3**, 1337. [DOI], [ADS]

Rabin, D., Jaksha, D., Kopp, G. and Mahaffey, C., 1992, "NIM — A Near Infrared Magnetograph", in *American Astronomical Society Meeting Abstracts*, Bulletin of the American Astronomical Society, 24, [ADS]

Stenflo, J. (Ed.), 1994, *Solar Magnetic Fields: Polarized Radiation Diagnostics*, Astrophysics and Space Science Library, 189. [ADS]

Sugar, J. and Corliss, C., 1985, *Atomic energy levels of the iron-period elements: Potassium through Nickel*. [ADS]

Wallace, L. and Livingston, W., 2003, *An atlas of the solar spectrum in the infrared from 1850 to 9000 cm-1 (1.1 to 5.4 micrometer)*. [ADS]

Wallace, L. and Livingston, W. C., 1992, *An atlas of a dark sunspot umbral spectrum from 1970 to 8640 cm(-1) (1.16 to 5.1 [microns])*. [ADS]

Wallace, L., Hinkle, K. and Livingston, W. C., 2002, *Sunspot umbral spectra in the regions 1925 to 2226 and 2392 to 3480 cm(-1) (2.87 to 4.18 and 4.48 to 5.35 [microns])*. [ADS]

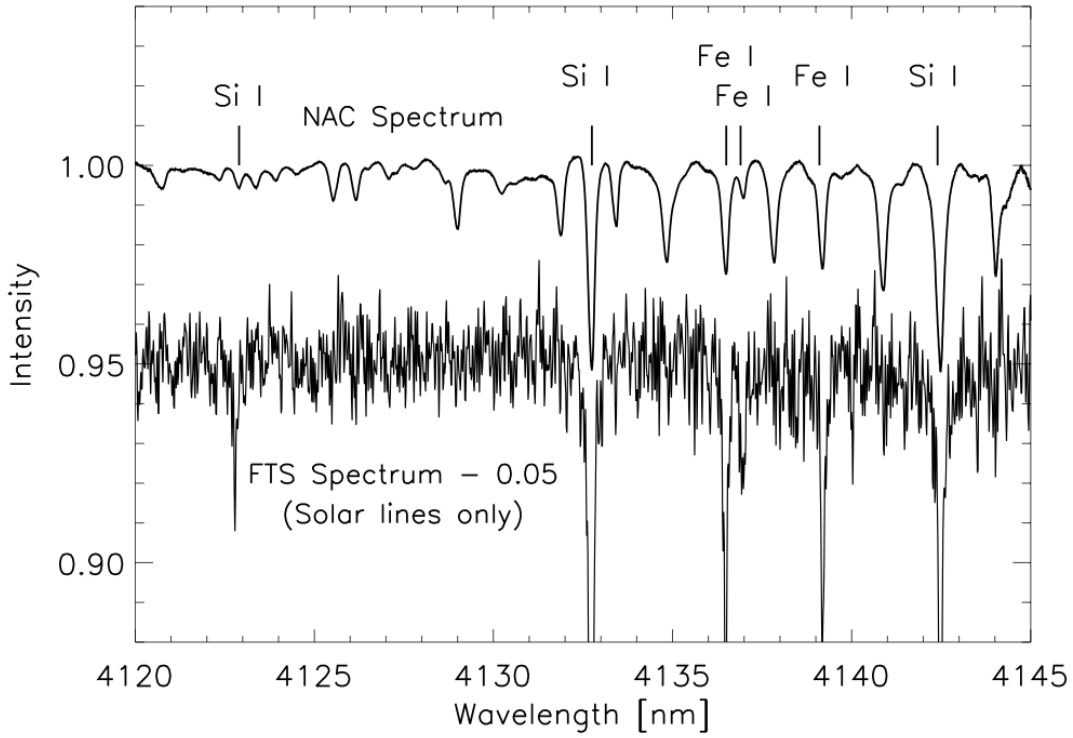


Figure 1: Intensity spectrum near 4135nm. The top plot represents the NAC spectrum, the bottom one is the FTS spectrum, offset by a small amount.

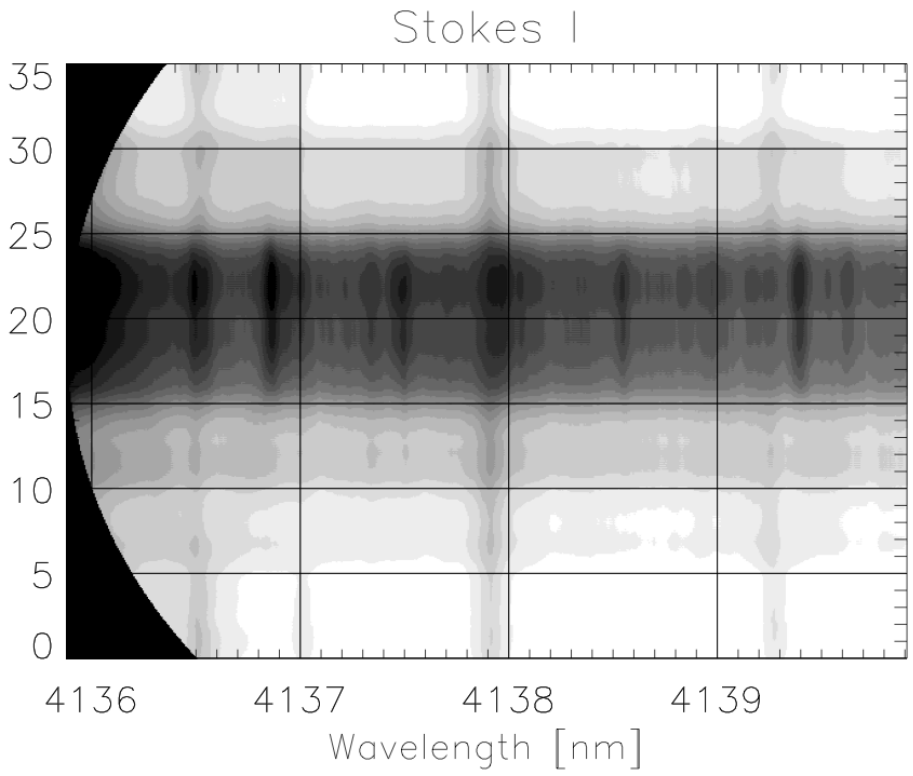


Figure 2: Intensity spectral frame from sunspot observations near 4135nm.

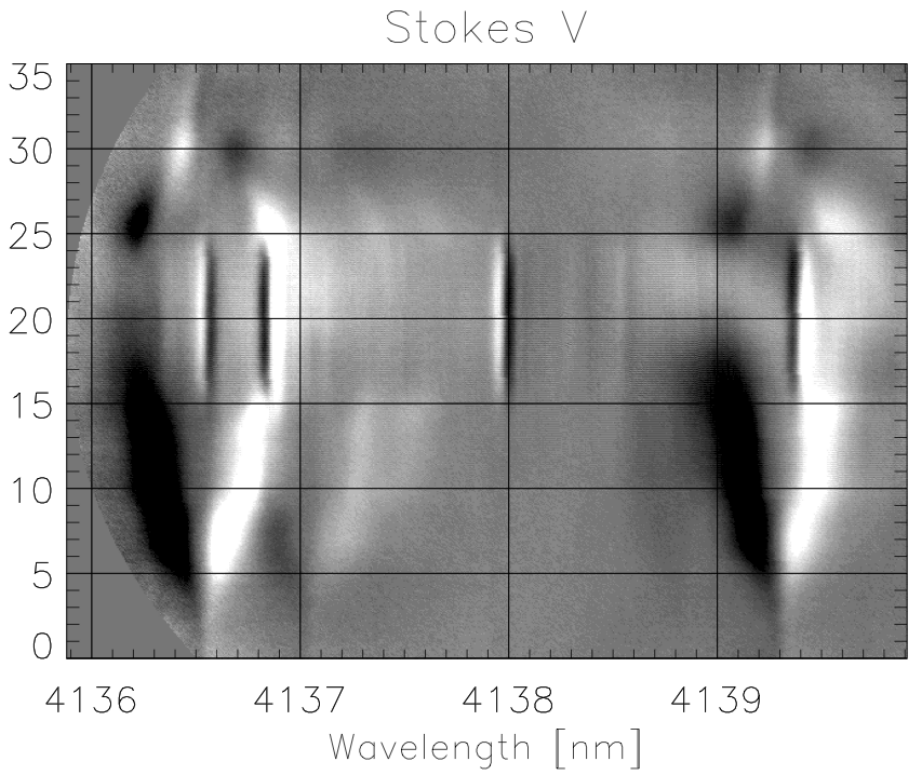


Figure 3: Stokes V spectral frame from sunspot observations near 4135nm.